Breaking Probability for Dominant Waves on the Sea Surface

MICHAEL L. BANNER

School of Mathematics, The University of New South Wales, Sydney, Australia

ALEXANDER V. BABANIN AND IAN R. YOUNG*

School of Civil Engineering, University College, The University of New South Wales, Canberra, Australia

(Manuscript received 30 March 1999, in final form 22 February 2000)

ABSTRACT

The breaking probability is investigated for the dominant surface waves observed in three geographically diverse natural bodies of water: Lake Washington, the Black Sea, and the Southern Ocean. The breaking probability is taken as the average number of breaking waves passing a fixed point per wave period. The data covered a particularly wide range of dominant wavelengths (3–300 m) and wind speeds (5–20 m s^{-1}). In all cases, the wave breaking events were detected visually. It was found that the traditional approach of relating breaking probability to the wind speed or wave age provided reasonable correlations within individual datasets, but when the diverse datasets are combined, these correlations are significantly degraded.

Motivated by the results of recent computational studies of breaking onset in wave groups, the authors investigated the hypothesis that nonlinear hydrodynamic processes associated with wave groups are more fundamental to the process of breaking than previously advocated aerodynamic properties, such as the wind speed or wave age. Further, these computational studies suggest that the significant wave steepness is an appropriate parameter for characterizing the nonlinear group behavior.

Based on this approach, analysis of the data revealed that the probability of dominant wave breaking is strongly correlated with the significant wave steepness for the broad range of wave conditions investigated. Of particular interest is a threshold of this parameter below which negligible dominant wave breaking occurs. Once this threshold is exceeded, a near-quadratic dependence of the breaking probability on the significant wave steepness was observed, with a correlation coefficient of 0.78. The inclusion of parameters representing the secondary influence of wind forcing and background current shear improved the correlation only marginally to 0.81.

The applicability of the breaking probability dependence found for the dominant waves was investigated for higher-frequency bins up to twice the spectral peak frequency f_p. The Black Sea data were used for this analysis, in which shorter breaking wave statistics were also measured. It was found that the maximum of the composite breaking frequency distribution gradually shifts from about $1.6 f_p$ for lower values of the peak steepness parameter to f_p for higher values of this parameter. The breaking probability in a comparable higher frequency band has a similar dependence on significant steepness to that found for the dominant waves.

1. Introduction

Breaking of the dominant waves on the sea surface is responsible for a local rapid loss of wave energy accumulated over long fetches under prolonged wind action. Knowledge of the occurrence and strength of these breaking events has important scientific and practical applications. Whitecapping due to wave breaking is a fundamental source term in the numerical prediction of sea state using the spectral wave energy balance equation, while in coastal and offshore engineering the impulsive forcing and subsurface turbulent mixing due to large-scale breaking wave events are of central importance in structural loading and safety.

Our present knowledge of breaking wave statistics and the related spectral dissipation source function for wave modeling is fragmentary. The strongly intermittent and nonlinear character of the breaking process creates profound complications for theoretical approaches to these problems. At the same time, field observations of breaking waves encounter logistical difficulties since the most important situations of extreme seas are usually the least accessible to systematic measurement. Even when reliable wave height data are obtained, the absence of established breaking criteria in such measurements makes it difficult to detect particular breaking events within these data records.

* Current affiliation: Faculty of Engineering, Computer and Mathematical Sciences, University of Adelaide, Adelaide, Australia.

Corresponding author address: Prof. Michael L. Banner, School of Mathematics, The University of New South Wales, Sydney 2052, Australia.
E-mail: m.banner@unsw.edu.au

In wave modeling, three major identified problems can be associated with wave breaking: (i) breaking criteria for an individual wave within a wave group, (ii) statistics of breaking events in relation to wave characteristics and environmental forcing, and (iii) the spectral source term for dissipation due to breaking. Although subject to intensive theoretical and experimental research effort for several decades, each of these problems has resisted fundamental progress (e.g., see Banner and Peregrine 1993). This is particularly apparent for ocean waves with their continuous spectra, pronounced group structure, and varying wind forcing levels. In this paper, we focus on the second issue (ii), primarily in regard to the dominant ocean waves. We also report on an initial examination of breaking probability of waves in spectral bands above the spectral peak. In this paper, breaking probability for the dominant waves is characterized by the mean passage rate past a fixed point of dominant breakers per dominant wave period, b_T. The dominant waves are assumed to have frequencies within $\pm 30\%$ of the spectral peak frequency. This conforms to the peak enhancement region adopted by Hasselmann et al. (1973) in JONSWAP and allows for wave groups comprising two or more waves. Thus b_T is the average fraction of dominant wave crests that break at any given point on the sea surface. This definition may be extended, in principle, to any spectral band above the spectral peak.

Following a concise overview of the literature, we present the results of our analysis of wave breaking datasets from three diverse field sites. First, we follow the traditional approach of relating breaking probability to atmospheric forcing. Using the same datasets, we then describe our results using an alternative primary dependence. The latter appears to provide a far more consistent correlation of dominant wave breaking probability.

a. Previous studies of wave breaking probability

Measurement of the breaking probability of dominant ocean waves is a challenging task, particularly when carried out by unattended instruments in the open ocean. Here, there is no consensus on exactly which properties need to be measured to provide unambiguous results on the occurrence and scale of the breaking waves. Identifying which environmental variables determine the breaking probability has been even more elusive.

While visual recording of wave breaking occurrence is arguably the most reliable method, other methods have been reported in the literature based on measurements of surface elevation, velocities, and accelerations. Various signal-processing techniques have been explored to extract breaking occurrences from such wave records, including Fourier and wavelet analysis. Other detection methods have used measurements of void fraction, whitecap coverage, subsurface turbulence, underwater sound, infrared properties of the surface, and microwave backscatter. Reconciling different sets of observations is complicated by the lack of overlap among the various techniques. Finally, we note that both wave field parameters and wind parameters have been proposed as appropriate independent variables, as described below.

b. Wave-related dependence

Much attention has focused on the joint probability density of individual wave heights and periods. Underlying this approach is the notion of a critical local steepness, or crest acceleration, based on results for limiting steepness of *steady* irrotational waves by Stokes (1880). These kinematic aspects of breaking onset have been investigated experimentally by Longuet-Higgins (1986), among others, and have been extended by several authors. Snyder and Kennedy (1983) proposed a probability model for breaking in the spectrum based on a spectral interpretation of the crest acceleration threshold, involving a relationship between the breaking probability and the fourth spectral moment (the acceleration spectrum). In Kennedy and Snyder (1983) and Snyder et al. (1983), numerical simulations and a field experiment were undertaken to verify the model, with encouraging initial agreement found between their simulated results, field results, and the model predictions. The acoustic observations of Ding and Farmer (1994) also provided support for this breaking probability model, but with some uncertainty in the underlying model parameter α. This class of probability model was extended by Yuan et al. (1986) and Papadimitrakis et al. (1988), among others. A similarly based parameterization of breaking influence was proposed by Huang (1986), using as the primary independent variable the significant wave steepness parameter $\mathcal{S} = \langle \eta^2 \rangle / \lambda_0$, where $\langle \eta^2 \rangle$ is the mean square wave height and λ_0 is the dominant wavelength.

Other observational studies have investigated the use of a *local* wave steepness threshold. These studies indicate that this approach is not robust when applied to the onset of wave breaking at sea, where a rather diffuse separation between breaking and nonbreaking wave populations is observed on the basis of individual wave steepness. Holthuijsen and Herbers (1986) visually monitored wave breaking events that occurred at a wave-rider (acceleration) buoy in an open ocean field site. They detected wave breaking events over a wide range of length scales, and these were registered synchronously with the buoy signal. The joint probability analysis of heights and periods of breaking and nonbreaking waves showed considerable overlap and did not clearly resolve breakers on the basis of individual wave steepness. Other findings of this study were that the probability of breaking was correlated with wind speed, varying from 0.10 to 0.16 within the observed range of wind speeds of 8–12 m s^{-1}. Also, it was observed that two-thirds of the breaking waves were ob-

served to occur in one-third of the wave groups. Further, these authors reported that breaking occurred most commonly in the center of a group, highlighting the importance of groupiness in the breaking process. This confirmed the earlier findings of Donelan et al. (1972) that breaking was visually correlated strongly with wave group structure.

c. Dependence on wind forcing

Several studies using different breaking detection methods have attempted to establish a connection between breaking probability and various atmospheric forcing parameters. The earliest such studies were of a related quantity W, the percentage whitecap cover. A very strong wind speed correlation $W \sim U_{10}^{3.75}$ was proposed by Wu (1979). It should be noted, however, that W may be rather different from the dominant wave breaking probability because it integrates whitecap contributions of all wave scales and may include residual foam cover.

The field study of Thorpe and Humphries (1980) used a breaker detection scheme based on a jump in the surface slope associated with the leading edge of the spilling region. It is believed that this method primarily registers dominant wave breaking events. These authors showed a clear correlation between U_{10} and the number of breaking waves per wave period, but did not provide a quantitative relationship for the observed correlation. A similar wave breaking detection method was also used by Longuet-Higgins and Smith (1983). Their instrument operated in wind speeds ranging from 1 to 14 m s^{-1} and they reported breaking probabilities of up to a few percent. The breaking probability increased with wind speed and inverse wave age.

The laboratory study of Xu et al. (1986) reported that the breaking probability P (ratio between the number of breaking waves and the total number of waves examined) increased rapidly with wind velocity U and followed a power law $P = U^{2.2}$, with P reaching 100% at winds near 20 m s^{-1} in their wind wave tank. Their detection method based on a threshold of the temporal derivative of the wave height signal is considered to be unsuitable for field conditions involving a broad range of breaking wave scales.

Weissman et al. (1984) used the high-frequency spectral band (18–32 Hz) of fine wire wave probe records to quantify breaking wave occurrences for wind waves on Lake Washington. For a wind velocity of about 6 m s^{-1} at a fetch of 7 km, they found the probability of breaking P was 8.64% with a breaking rate of 17/km. In this approach, breaking of the different scales is not easily separated and the high signal bandwidth is not usually available in ocean wave records.

Katsaros and Atakturk (1992) used continuous video records of breaking event occurrences at their wire wave probe on Lake Washington. They correlated their results for spilling and plunging breakers using five different atmospheric parameters, both individually and in various combinations, for the dependence of breaking probability on wind forcing. They found the best correlation was 0.81 for the following fit to their data:

$$P = -2.47 + 32.87u_*^2 + 42.37\frac{u_*}{c_p},$$

where u_* is the friction velocity and c_p is the phase speed of waves at the spectral peak. In this correlation, the second term describes the influence of the wind stress and the third term reflects the stage of wave development. While there was no explicit information given on the range of scales of breaking waves, we associate the majority of their reported spilling and plunging wave breaking events with the dominant waves, as they reported microscale breaking statistics separately.

d. Other detection methodologies

There have been other closely related studies based on a range of conventional and innovative detection methods (e.g., Stolte 1994; Melville et al. 1992; Ding and Farmer 1994; Su et al. 1996; Bass and Hay 1997; Jessup et al. 1997; Gemmrich and Farmer 1999; among others), but these mostly have not provided breaking occurrence statistics for the dominant waves alone. An exception is the Ding and Farmer (1994) study that used a small array of four omnidirectional hydrophones deployed on a freely drifting float to map the location and movement of breaking waves in the ocean. Their technique detected the breakers and measured their propagation speed and geometrical evolution. Very recently, Gemmrich and Farmer (1999) described measurements of the scale and occurrence of breaking waves at sea for a wide range of conditions, based on void fraction conductivity measurements. They found that breaking probability was not highly correlated with either wind speed or wave age. Interestingly, during one deployment they observed that the breaking probability continued to increase after the wind had dropped from 17 to 7 m s^{-1}. Their observations did show a high correlation, however, when framed in terms of a relative wind input strength parameter that compares the wind input strength to that of a fully developed windsea at that wind speed.

From the literature, it is clear that there is little consensus on the environmental parameter or parameters that control the onset of breaking of the dominant waves. In this paper, we extend the discussion on this fundamental issue through our investigation of a diverse new dataset. Our analysis offers further confirmation that the traditional approach of relating breaking probability to the standard wind forcing parameters provides a relatively poor correlation when results are analysed for the broad range of wave conditions represented in our dataset. We then propose and investigate an alternate primary dependence for breaking probability of the dominant ocean waves based on the results of numerical

experiments on nonlinear wave group hydrodynamics. The theoretical background is summarized in the following section. As an extension of this approach, we report preliminary breaking statistics observed for frequency bands above the spectral peak and examine how closely breaking probability for a higher-frequency band conforms to the dependence observed for the dominant waves at the spectral peak.

2. Breaking dependence on wave group dynamics

Several researchers have documented a strong association of wave group structure with the onset of breaking of dominant waves. Donelan et al. (1972) reported observing up to several consecutive waves breaking at the peak of the group envelope before sufficient energy was lost from the group. Holthuijsen and Herbers (1986) found significant wave group influence in their open ocean study of wave breaking. When breaking occurred, the position of the first breaker in a group was slightly ahead of the center of the group. They concluded that the overall fraction of breakers occurring within wave group structures was close to 70%. Two-dimensional wave tank investigations and numerical model studies have also provided considerable insight into the key role of nonlinear wave group dynamics in the onset of breaking. The literature on this approach has been reviewed in Banner and Peregrine (1993) and more recently in Banner and Tian (1998). Here, we highlight only the results of most direct relevance to this paper.

Dold and Peregrine (1986, henceforth DP) used a fully nonlinear, two-dimensional, free surface computational model in a periodic domain to study the evolution of wave groups comprising a fundamental carrier wave with small upper and lower sideband components. As input parameters, they used the initial carrier wave slope $(ak)_0$ and the number of waves N in one modulation interval. They demonstrated that, for a given N, breaking always occurred above a threshold value of $(ak)_0$, and below this threshold, recurrence always ensued toward the original wave group. It is important to point out that this initial steepness threshold depends on N, the number of waves in the group, but that for $N > 4$ it varies only slowly.

More recent confirmation of the central role of nonlinear wave group dynamics is evident in the findings of several investigations. Banner and Tian (1998) studied the onset of wave breaking in unforced, nonlinear modulating wave groups. They investigated breaking onset in terms of the behavior of dimensionless growth rate parameters based on the relative rates of change of the local mean energy and momentum densities. The calculations were based on the DP free surface code used in conjunction with an interior irrotational flow code. Their results provided evidence for the complex evolution of the maximum of wave energy envelope where wave breaking is observed to occur as fast oscillations superposed on a slower mean evolution. This behavior is consistent with the observations reported earlier by Rapp and Melville (1990, Fig. 12). The results of such numerical and laboratory experiments indicate a range of local wave steepness values at the onset of breaking so breaking criteria based on a threshold value of local steepness do not appear to be well-founded.

Other possible factors influencing breaking onset

The wind drift, upper ocean shear, wind forcing, breaking-induced turbulence, and three-dimensionality have all been recognized as potentially important factors in influencing the onset of breaking. There is little available direct observational evidence of the importance of these factors, so we sought guidance from numerical simulations of idealized cases where possible. We used the DP code to examine cases of a superimposed linear shear layer considerably stronger than the levels recently reported by Terray et al. (1999) and found only a small ($<10\%$) reduction in the evolution time to breaking. We also found that that the influence of very strong wind forcing was not of primary importance for the evolution time to breaking. In one case, the time to breaking was reduced by 15%, while in another case, the wind forcing delayed the onset of breaking. While these model findings remain to be validated experimentally, they suggest strongly that nonlinear wave group dynamics is the primary mechanism involved. Another related influence is the background turbulence injected by the field of breaking waves. While central to the effective eddy viscosity in the surface layer (e.g., Craig and Banner 1994), its local influence on breaking onset is not known, but we anticipate this to be secondary. A more direct issue is three-dimensionality, as the dominant ocean waves have a small but finite directional spreading distribution and large whitecaps are often short-crested in appearance. A body of literature on three-dimensional effects is beginning to develop and recent laboratory investigations (e.g., Kolaini and Tulin 1995; She et al. 1997; Nepf et al. 1998) have quantified modest differences in breaking-related local steepness and energy losses between these short-crested wave trains and comparable two-dimensional wave trains. Nevertheless, it is apparent in all of these studies that the evolution to breaking is still underpinned by their nonlinear wave group behavior.

On this basis, we propose that the key factor associated with the onset of wave breaking is nonlinear momentum and energy transfer within wave groups with direct wind forcing, shearing current influence, and three-dimensionality of secondary importance. This approach suggests an alternative basis for parameterizing the environmental dependence of the average dominant wave breaking probability in terms of the nonlinearity of the wave field. We look to the available field data described in section 3 for observational support for these ideas and for a suitable environmental parameterization in section 4.

TABLE 1. Summary of the 10-m mean wind speed U_{10}, significant height H_s of the windsea, spectral peak frequency f_p, significant spectral peak steepness ε, shear parameter Δ, wave age parameter γ, and spectral peak breaking probability b_T for the Black Sea data. The symbols are defined in section 4b of the text. Numbers in parentheses indicate corresponding record numbers used in Fig. 8.

Run	U_{10} (m s^{-1})	f_p (Hz)	H_s (m)	ε	Δ	γ	b_T
6 (1)	11.7	0.36	0.39	0.085	0.318	0.430	0.038
7 (2)	12.7	0.34	0.49	0.099	0.280	0.441	0.065
9 (3)	14.0	0.30	0.53	0.080	0.336	0.428	0.060
10 (4)	14.4	0.31	0.54	0.084	0.341	0.455	0.052
11 (5)	15.0	0.44	0.38	0.120	0.344	0.657	0.063
13 (6)	14.6	0.39	0.45	0.114	0.320	0.581	0.067
14 (7)	13.7	0.41	0.45	0.126	0.285	0.571	0.084
16	8.4	0.17	1.19	0.062	0.148	0.146	0
18	11.2	0.16	1.32	0.058	0.198	0.183	0
211	9.5	0.16	0.83	0.032	0.303	0.154	0
238	10.7	0.17	0.89	0.040	0.293	0.186	0
242 (8)	10.0	0.27	0.99	0.124	0.139	0.274	0.034
244 (9)	8.7	0.25	0.88	0.093	0.152	0.224	0.058

3. The measurements

In this paper, we use deep water datasets from three field sites that provide a wide range of dominant wave frequencies: the Black Sea ($f_p = 0.2$–0.4 Hz), the Southern Ocean ($f_p < 0.1$ Hz), and Lake Washington ($f_p > 0.5$ Hz). The 10-m reference wind speed U_{10} ranged from 3 to 20 m s^{-1}.

a. Black Sea data

This section reports the results of a comprehensive wave breaking analysis of Black Sea data. The experimental arrangement involved visual surveillance of waves passing over a wave probe, with collocated breaking events labeled electronically by an observer. With this data we were able to investigate the distribution of breaking probability with respect to the distance from the spectral peak. The first 12 records (Table 1) were obtained in 1993 during the 31st cruise of the R/V *Professor Kolesnikov* (henceforth *PK*) operated by the Marine Hydrophysical Institute (MHI) in Sebastopol. The last four records are from the 1986 field experiment conducted by the Air–Sea Interaction Department at MHI.

The *PK* wave data were recorded using an accelerometer buoy, as described by Babanin et al. (1993). Briefly, the buoy diameter was 0.58 m and its operational bandwidth was 0.08–1.0 Hz, which easily covered the wave frequencies of interest. It was deployed around 100 m from the ship to avoid any interference between the ship and the wind and wave fields. Record lengths of 34 min to 68 min were acquired using a sampling frequency of 4 Hz. One of the authors (AVB) observed the buoy from the vessel and triggered an electronic signal to register the passage of a whitecap over the buoy. This signal was recorded synchronously with the buoy data. The observer varied the duration of the electronic label according to the geometrical size of the whitecap, providing an approximate indication of individual breaker dimensions for future analysis. The observer was about 10 m above sea level, allowing a clear view of whitecaps with scales down to the size of the buoy. The environmental data collected simultaneously included 10-min averages of the 10-m wind speed and direction, measured by a standard Russian M63-MP anemometer on the ship's bow, together with mean water and air temperature data.

The first 10 records were obtained with the ship anchored about 3.2 to 6.4 km offshore on the relatively flat west coast of the Crimea. Relatively young, strongly forced, fetch-limited waves with $U_{10}/c_p = 2.7$–4.1 were observed. Their spectral peak frequencies f_p ranged from 0.3 to 0.44 Hz. The wind speed U_{10} ranged from 11.7 to 15.0 m s^{-1}. Records 16 and 18 were gathered from the drifting vessel during the same *PK* cruise in the Eastern Mediterranean Sea, during which older waves were observed approaching full development, with $U_{10}/c_p = 0.9$ and 1.15. Their rather low observed peak frequencies of 0.16 and 0.17 Hz corresponded to 8.4 and 11.2 m s^{-1} wind speeds respectively. The last four wave records were recorded from an oil rig situated 60 km offshore in the northwest region of the Black Sea in horizontally uniform water of 30-m depth. The four-wire (0.3-mm diameter nichrome) directional array wave gauge used to collect the wave data, as well as the platform and its location, are described in detail by Babanin and Soloviev (1998a,b). The wave sensors had a linear regression between readings and water level accurate to within 1% of the greatest deviation and were able to resolve wave frequencies up to approximately 10 Hz. The wave gauge was located about 15 m away from the nearest platform leg and only waves unperturbed by the platform influence were recorded. For records 211 through 244, the fetch exceeded 400 km and was practically unlimited. The records were 12.5 min long and were recorded using a sampling interval of 0.05 min. The observer located 16 m above the wave probe array monitored one of the wave probes and triggered a signal whenever a whitecap of any size occurred at the probe. The wind wave data, obtained with much higher frequency resolution than previous records, embraced moderate to well-developed waves with peak frequencies $f_p = 0.16$–0.27 Hz, wind speeds $U_{10} = 8.7$–10.7 m s^{-1}, and wave development stages $U_{10}/c_p = 1.0$–1.7. The complete environmental dataset included 1-min averaged wind speeds, 5-min averaged surface current speed, and direction measurements at 3-h intervals (Babanin 1988), as well as water and air temperatures recorded every 3 hours. To avoid possible airflow distortion by the platform, an M63-MP anemometer was deployed on a tower 42 m above sea level, well above the deck buildings. The drag coefficient correlation of Large and Pond (1981) was used to estimate the 10-m wind speed from the observed data.

The surface elevation time series with labeled indi-

TABLE 2. Summary of the parameters of the Southern Ocean dataset (same symbols as in Table 1).

Run	U_{10} (m s^{-1})	f_p (Hz)	H_s (m)	ε	Δ	γ	b_T
10	19.8	0.074	9.2	0.083	0.124	0.142	0.027
11	16.0	0.083	4.2	0.050	0.190	0.131	0

vidual breaking events were analyzed to determine individual breaker properties and breaking statistics. The accelerometer data series from the *PK* cruise were segmented to reduce the effects of low-frequency trends and integrated twice prior to analysis. With shorter waves riding on longer ones, occasional confusion could occur as to which wave scale was actually breaking but, since dimensional information on the individual whitecaps was available from the label length, we believe that uncertainties of this type were negligible.

b. The Southern Ocean data

This dataset was obtained during the Southern Ocean Waves Experiment (SOWEX) staged in June 1992 (see Banner at al. 1999). Nadir-look video images of the ocean surface were recorded from a research aircraft flown upwind at altitudes of 680 m (10 June) and 250 m (11 June) over the Southern Ocean 225 km southwest of Tasmania. The video frame digitization resolved 320 $\times$ 200 pixels, providing spatial resolutions of 1.62 m/pixel and 0.59 m/pixel, respectively. Table 2 provides a summary of the experimental conditions.

A video recorder interfaced to a personal computer was programmed to play back an assigned number of sequential video frames. During the processing, the software digitized these frames and counted the number of pixels in each whitecap. The number of breakers passing through a chosen point on the screen was counted and estimates were made of the distances and travel time of these breakers. After correction for the wind and aircraft velocities, the phase speeds and frequencies of the breakers were calculated. We only considered breakers propagating with speeds close to the phase speed of the spectral peak. The methodology is very time consuming and only one representative breaking probability was obtained for each day. This was the only way to include breaking statistics for the very long Southern Ocean waves, consistent with our goal of including the widest possible range of wavelengths.

The processed video segments were 5 and 9 min long, respectively, consistent with the duration of the steady upwind flight legs at constant aircraft altitudes and representing approximately 30 and 40 min records at a fixed point. The peak frequencies of 0.083 and 0.074 Hz have wavelengths of 220 m and 290 m, respectively. Corresponding to the prevailing 10-m wind speeds of 16 m s^{-1} and 20 m s^{-1}, these waves were nominally just below and just above the fully developed Pierson–Moskowitz (1964) state. Further details on the SOWEX instrumentation are given in Banner et al. (1999).

c. Lake Washington data

The Lake Washington dataset, described by Katsaros and Atakturk (1992), represents the other extreme of natural deep water wind waves with very short wavelengths. These short fetch-limited waves were generated by light winds. For this dataset, U_{10} ranged from 3.4 to 6.8 m s^{-1}, with peak wave frequencies $f_p = 0.55$ to 0.75 Hz and wave development stages of $U_{10}/c_p = 1.5$ to 2.5. The waves were measured using a wire wave gauge, with breaking events recorded by a video camera observing the wave gauge. A detailed analysis provided the number of plunging, spilling, and microscale breakers for each of the sixty-six 17-min records. In the present paper, we combined the available plunging and spilling breaker statistics to quantify the breaking waves in the spectral peak band.

4. Breaking probability of the dominant waves

As defined above, breaking probability b_T for the dominant waves is the mean passage rate past a fixed point of dominant wave breaking events per dominant wave period. The dominant waves are taken within the spectral band of 0.7 f_p to 1.3 f_p, which contains the spectral components determining the group structure of the dominant wave field. Measurement of b_T requires averaging over a large number of wave groups since the breaking process is characterized by long-period intermittencies, as observed both in this study and in earlier studies by Holthuijsen and Herbers (1986) and Babanin (1995).

As discussed earlier, wave breaking properties such as breaking probability, whitecap area coverage, etc., have been assumed to have a primary dependence on the wind speed U ranging from linear up to fourth power. In Fig. 1, breaking probabilities for the present datasets are plotted against the 10-m wind speed U_{10}. It is seen in Figs. 1a and 1b that, in isolation, the Black Sea data and the Lake Washington data correlate rather well with U_{10}. When these two datasets are plotted together in Fig. 1c, however, they are seen to have distinctly different offsets, while the two Southern Ocean data points show yet another dependence on U_{10}. We concluded that it was not possible to establish a common dependence of the dominant wave breaking probability on U_{10}.

In Fig. 2, the breaking probability was plotted against another plausible wind forcing parameter, the inverse wave age U_{10}/c_p. Here it is seen that the individual datasets, despite having similar offsets, have different rates of change of breaking probability with wave age. This is the drawback of wave age as the primary controlling parameter, but we do retain it as a potentially relevant auxiliary variable in the subsequent analysis.

The present attempt to improve the parameterization

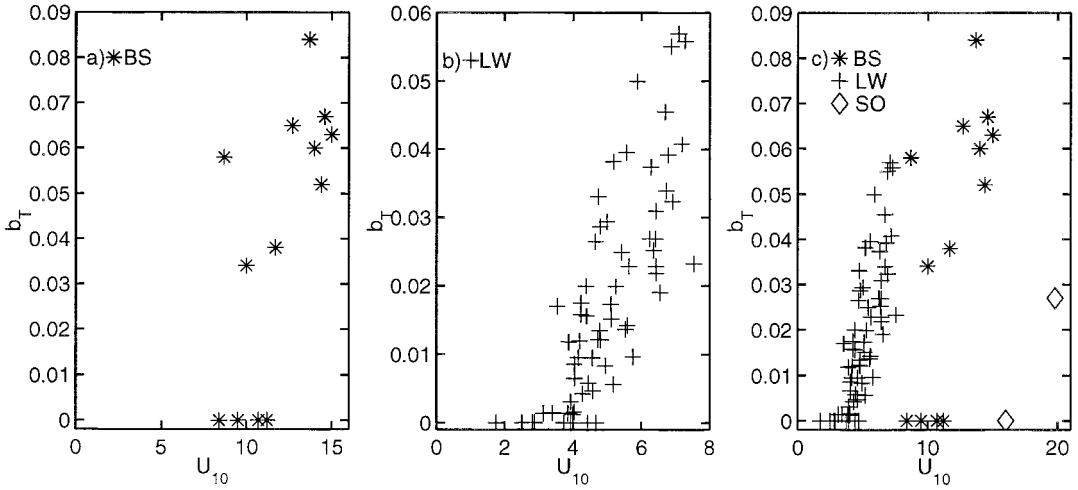

FIG. 1. Plot of observed dominant wave breaking probability b_T vs 10-m wind speed U_{10} for three diverse field sites: (a) Black Sea data (*), (b) Lake Washington data (+), and (c) composite of Southern Ocean data (◇) with (a) and (b).

of dominant wave breaking probability is based on insight provided by the numerical calculations of the evolution to breaking of two-dimensional nonlinear deep water wave groups by Dold and Peregrine (1986), Banner and Tian (1998), and our more recent unpublished calculations discussed above. We proceed from the hypothesis that the dominant ocean waves, with their narrow directional spreading, reflect the behavior observed in these numerical calculations. Our assessment of the relative importance of nonlinear group dynamics, vertical shearing currents, and wind forcing by surface pressure in phase with the carrier wave slope indicates that the nonlinear dynamics associated with the wave group structure appears to be the dominant influence in the onset of wave breaking. In the following section, we describe how this complex hydrodynamical process underlying breaking onset may be parameterized primarily in terms of the mean steepness of the dominant wave field.

a. Dependence on the dominant wave steepness

To address the primary goal of this study, a parameter was needed that reflected the fundamental role of nonlinear group dynamics in determining breaking onset. Since the present focus is on mean breaking characteristics, it was very desirable to be able to relate this parameter to standard properties of wave fields, such as wave height spectra.

One parameter of immediate relevance in characterizing group properties is the nondimensional spectral

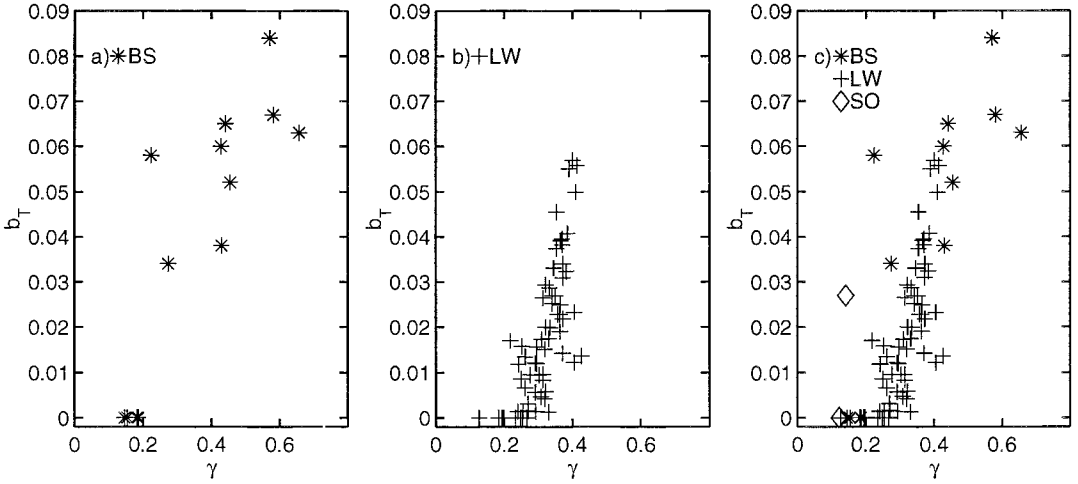

FIG. 2. Plot of observed dominant wave breaking probability b_T vs wave development parameter γ for three diverse field sites: (a) Black Sea data (*), (b) Lake Washington data (+), and (c) composite of Southern Ocean data (◇) with (a) and (b).

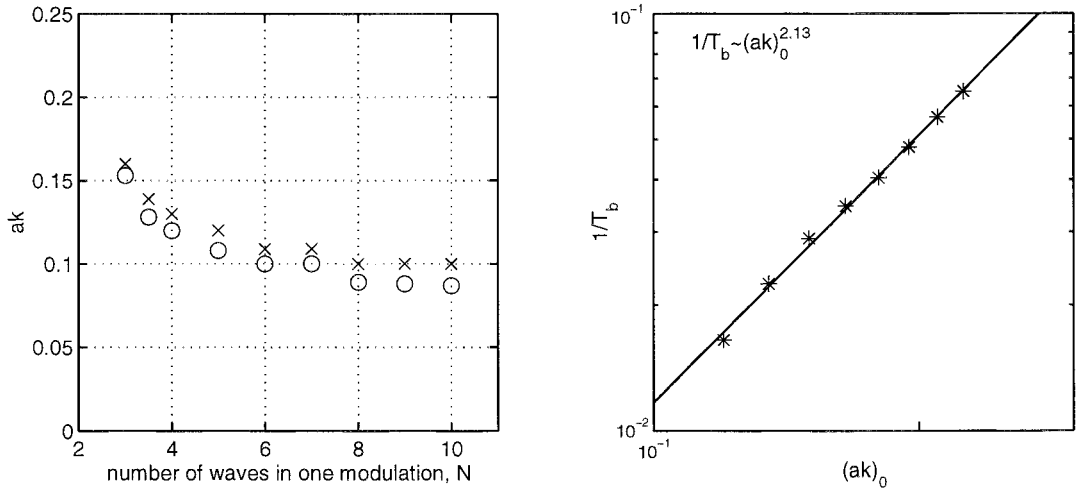

FIG. 3. (a) Dependence of evolution to breaking or recurrence on initial carrier wave steepness $(ak)_0$ predicted by the DP86 numerical model: ○ indicates upper bound for evolution to recurrence; x indicates lower bound for evolution to breaking. (b) Near-quadratic dependence of the reciprocal of the number of carrier wave periods to breaking as a function of the initial carrier wave steepness $(ak)_0$

bandwidth parameter ν (Longuet-Higgins 1984), defined by

$$\nu^2 = m_2 m_0 / m_1^2 - 1,$$

where m_i is the spectral moment of order i given by $m_i = \int_0^\infty \omega^i F(\omega)\, d\omega$ (F is the frequency spectrum). In practice, bandpass filtering of the wave record is necessary and ν depends on the spectral bandwidth: Longuet-Higgins (1984) found that upper and lower cutoffs at $1.5 f_p$ and $0.5 f_p$ were the most suitable. While intuitively attractive, the potential link between ν and the probability of wave breaking is not yet established by any dataset and needs to be investigated further.

As discussed earlier in section 2, DP reported the existence of an initial carrier wave steepness threshold that separates wave groups that evolve to breaking from those that undergo recurrence without breaking. Their result, reproduced in Fig. 3a, shows that the breaking/recurrence threshold depends on the number of waves N in the group, although this dependence is seen to be relatively modest beyond $N = 3$. On the other hand, the Banner–Tian growth rate parameters have a threshold that appears to be less sensitive to N. However, it is not possible to determine these parameters from routinely available wave data.

Based on these considerations, we investigated the potential suitability of the significant wave steepness at the spectral peak as the primary parameter associated with the onset of dominant wave breaking. Using the DP code, we computed T_b, the time to breaking onset from an initial nearly uniform wave group configuration, as a function of initial steepness $(ak)_0$ for $N = 5$. This result is shown in Fig. 3b. We concluded that initial steepness $(ak)_0$ had the strongest influence on T_b, with the inverse time to breaking almost quadratically dependent on $(ak)_0$. We also found that for a given initial steepness of 0.12, T_b was insensitive to the choice of N for $N \geq 5$. As discussed in section 1, the influence on T_b of other possible variables such as the strength of wind forcing and background shear was also found to be secondary. Our computational approach is based on investigating the time to breaking of a *quasi-uniform* wave group. Clearly, this class of initial condition is not realizable in open ocean situations, so our results on the behavior of T_b are only intended to be suggestive of potential dependences for open ocean correlations.

We conjectured that the stochastic nature of group lengths in ocean waves should average out the variation with N of the hypothetical critical initial steepness suggested by the numerical experiments as exerting an underlying influence on the onset of breaking. This behavior is paralleled in laboratory wave tank experiments, for example, Rapp and Melville (1990). This led us to propose its counterpart for real ocean waves: a significant spectral peak slope threshold based on the observed wave spectrum. We note that Huang (1986) previously used a closely related parameter, the significant wave slope, in his modeling of breaking influence on upper ocean dynamics.

b. *Definitions of key breaking wave parameters*

The breaking of local wind-generated seas often takes place in the presence of low steepness background swells from distant storms, and we assume here that these low steepness swell waves have little effect on the dynamics of breaking events of the dominant local wind sea. Hanson and Phillips (1999) describe how the swell contributions may be filtered out to provide the significant wave height of the local wind sea.

A significant wave steepness may be derived simply from $H_s k_p/2$, where $H_s = 4\sqrt{m_0}$ is the significant wave

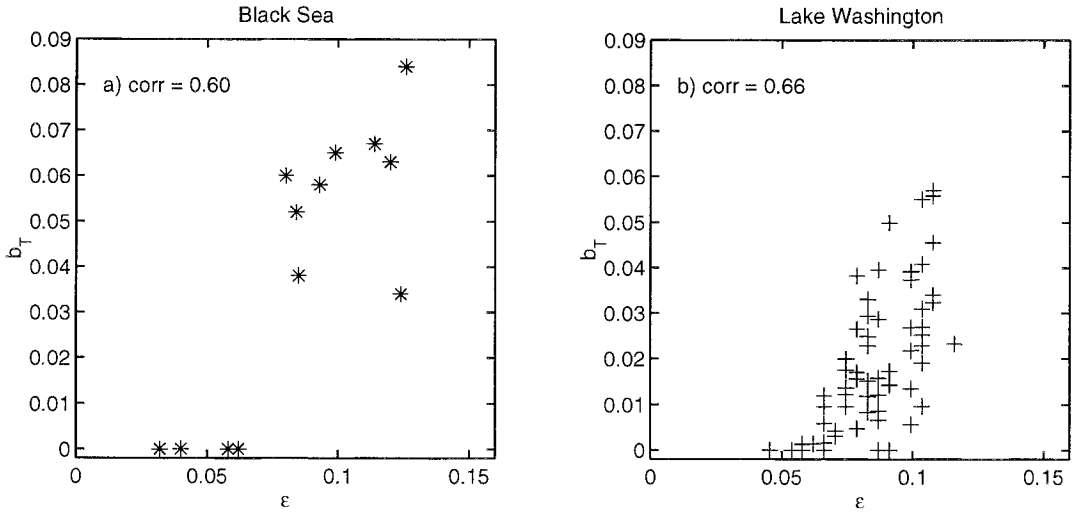

FIG. 4. Plot of observed dominant wave breaking probability b_T vs the dominant wave steepness ε for two diverse field sites: (a) Black Sea data (*), and (b) Lake Washington data (+). The legend shows the correlation coefficient based on a linear fit.

height of the local wind sea and k_p is its spectral peak wavenumber. This steepness measure, however, contains some contribution from the shorter, higher-frequency wind wave components. Thus, for our present purpose, we can conveniently define the significant spectral peak steepness of the local wind sea by

$$\varepsilon = \frac{H_p k_p}{2}, \tag{4.1}$$

where

$$H_p = 4\left\{\int_{0.7f_p}^{1.3f_p} F(f)\, df\right\}^{1/2}.$$

Here $F(f)$ is the frequency spectrum of the windsea after filtration of any background swell. We propose that ε is an appropriate parameter as it not only reflects the mean steepness of the dominant waves, but also provides a measure of their nonlinearity. Its suitability as a measure of nonlinear energy flux within dominant wave groups and breaking onset is assessed below.

5. Results

Figure 4 shows the number of breakers per wave period as a function of the dominant wave steepness ε for the Black Sea data (Fig. 4a) and Lake Washington data (Fig. 4b). Two conclusions may be drawn from these results. First, these figures show that steeper dominant waves have higher breaking probabilities and these are well correlated with the spectral peak steepness parameter ε. Second, there is strong visual evidence of a threshold value for ε around 0.05–0.06 that determines whether dominant wave breaking occurs or not. This level is consistent with the threshold level of $(ak)_0 \sim 0.1$ reported in the DP calculations once this is converted to an equivalent root mean square measure and account is taken of the group structure. We note in passing that the proposed ε threshold differs from a conventional breaking criterion as it is based on wave spectral information rather than individual wave characteristics; also, individual wave breaking criteria do not determine how many waves break once the threshold is exceeded.

a. Dependence on surface shear

A wind-driven vertical shear current is usually present in the ocean, but its magnitude and depth distribution is a complex research issue (e.g., Craig and Banner 1994). The results of Teles da Silva and Peregrine (1988), Millinazzo and Saffman (1990), Banner and Tian (1998), among others, suggest that a background linear vertical shear current should have a dynamical influence on the evolution to breaking of a deep-water gravity wave train. Banner and Tian (1998) reported that the presence of a superposed linear vertical shear current contributes to breaking onset by marginally reducing the time to breaking. The actual wind-induced surface layer shear is a complex and elusive region for reliable measurements because of the presence of the orbital motions of surface waves as well as the breaking-induced current shear (Terray et al. 1999). For the purpose of the present paper, we seek a surface shear measure that has the correct order of magnitude and is readily estimated from routine measurements. We proceeded from the recent PIV wind wave measurements of Peirson and Banner (1999, manuscript submitted to *J. Fluid Mech.*), who reported typical values of the surface drift to wind friction velocity $u_s/u_* \sim 0.03$, exclusive of the Stokes drift contribution. Based on typical corresponding U_{10} levels, we adopted a representative magnitude for the surface layer *wind-induced* current $u_s \sim 0.01U_{10}$.

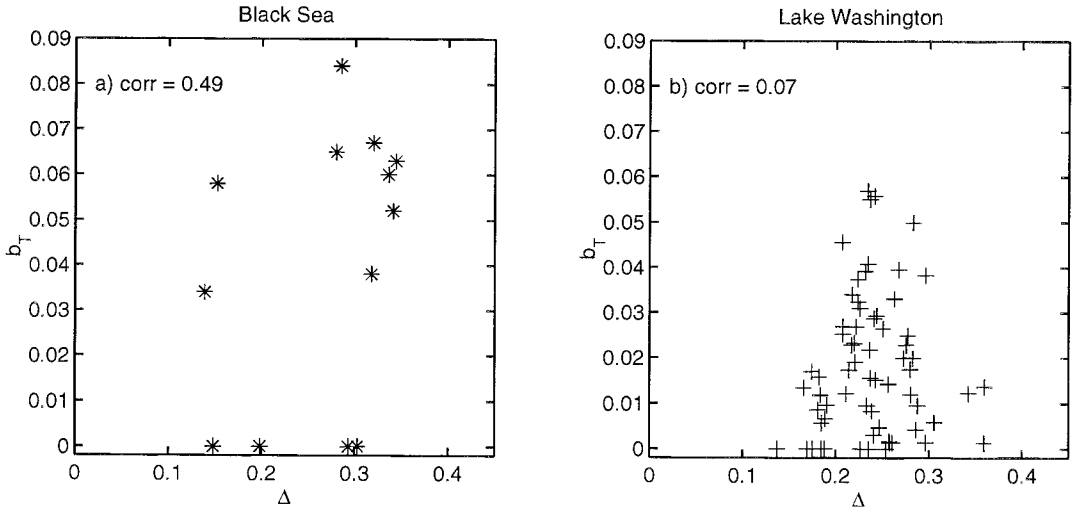

FIG. 5. Plot of observed dominant wave breaking probability b_T vs surface shear parameter Δ for two diverse field sites: (a) Black Sea data (*) and (b) Lake Washington data (+). The legend shows the correlation coefficient based on a linear fit.

As our indicative [$O(0.1)$] shear influence parameter for the wave field, we chose the ratio of the wind-induced surface current u_s to maximum orbital velocity u_o of a linear surface gravity wave with height equal to the significant wave height H_s:

$$\Delta = \frac{u_s}{u_o} = \frac{0.01U_{10}}{\varepsilon c_p}.$$

The Black Sea and Lake Washington breaking wave datasets plotted in Figs. 5a,b show that the breaking fraction increases with the shear parameter, although with a far lower visual correlation than seen for the peak steepness. Also, the existence of a shear threshold is not as evident as with the steepness. These conclusions are consistent with the secondary role of vertical shear reported in the numerical computations discussed above. To reflect this possible secondary dependence, we retain Δ as a potentially important variable in the ensuing analysis through an assumed linear perturbation term of the form $(1 + \Delta)$.

b. Dependence of the breaking probability on the wind forcing strength

The dependences of breaking probability on wind speed and on wave age alone were shown in Figs. 1 and 2. Our unpublished numerical experiments with wind forcing indicate that it has only a secondary impact on the calculated time to breaking relative to the unforced case when only nonlinear interactions were operative. We therefore chose to incorporate the wind forcing dependence through an assumed linear perturbation term of the form $(1 + \gamma)$, where $\gamma = U_{10}f_p/g$ is an inverse wave age parameter with a dynamic range from 0 to ~0.5 for field conditions. We note, however, that for very strongly forced conditions such as occur in wind wave tanks, this parameter can become significantly larger than 1. For such strongly forced conditions, the fractional rate of addition of momentum from the wind can be substantial and the primary dependence on hydrodynamic forcing may not be valid for such conditions.

c. Overall dependence for the combined datasets

In this section we examine how well the diverse datasets from the three measurement sites conform to the proposed parameterisations.

First, the composite data dependence on the dominant wave steepness ε alone is shown in Fig. 6 using log–log axes to highlight visually any power law behavior. Note that this plotting format suppresses all data points with zero breaking probability. The fit to the diverse dataset is very encouraging and the legend shows the best-fit statistics using a standard analysis with the ordinate data taken as the independent variable. This approach was motivated by our belief that the determination of the number of observed breaking events had intrinsically less error than the spectral peak steepness determination. In any event, this method gave a better visual fit to the data. The overall correlation was found to be close to quadratic, with a correlation coefficient of 0.78.

Second, for the combined dataset, the dependence of the spectral peak breaking probability on the composite steepness/wind-forced shear parameter $\varepsilon(1 + \Delta)(1 + \gamma)$ is shown in Fig. 7. This combined parameter incorporates the observed trends of breaking probability primarily on the spectral peak steepness with a secondary dependence on the surface layer shear and wind forcing

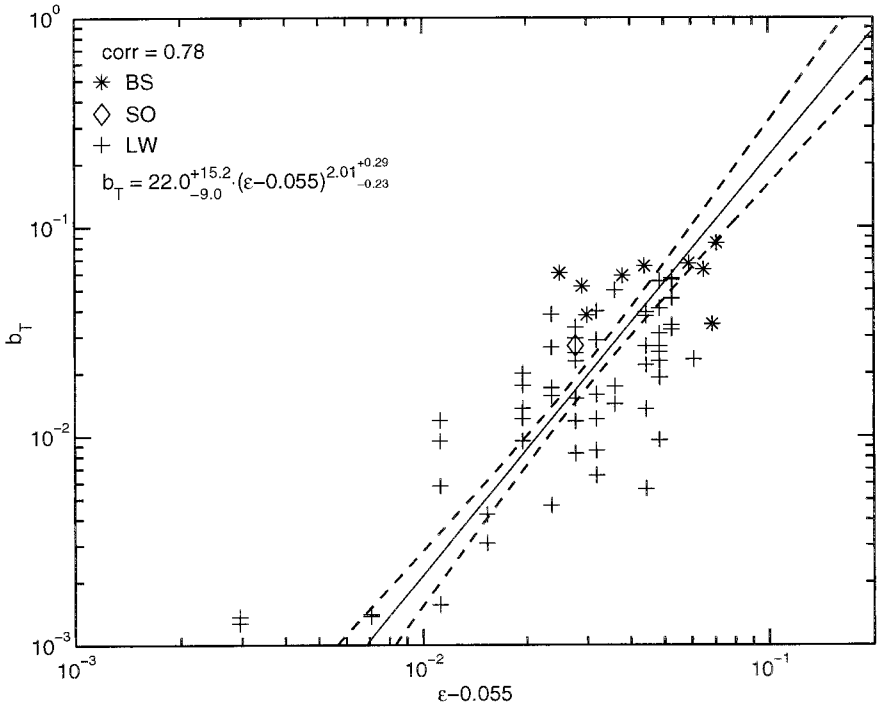

FIG. 6. Composite log–log plot of the observed dominant wave breaking probability b_T vs the modified dominant wave steepness ($\varepsilon - 0.055$) for three diverse field sites. The offset level of 0.055 is the mean peak steepness threshold below which negligible breaking was observed: (a) Black Sea data (*), (b) Lake Washington data (+), and (c) Southern Ocean data ($\diamond$). The legend shows the correlation coefficient based on a linear best fit in the log–log domain, together with the coefficients at the ±90% confidence limits.

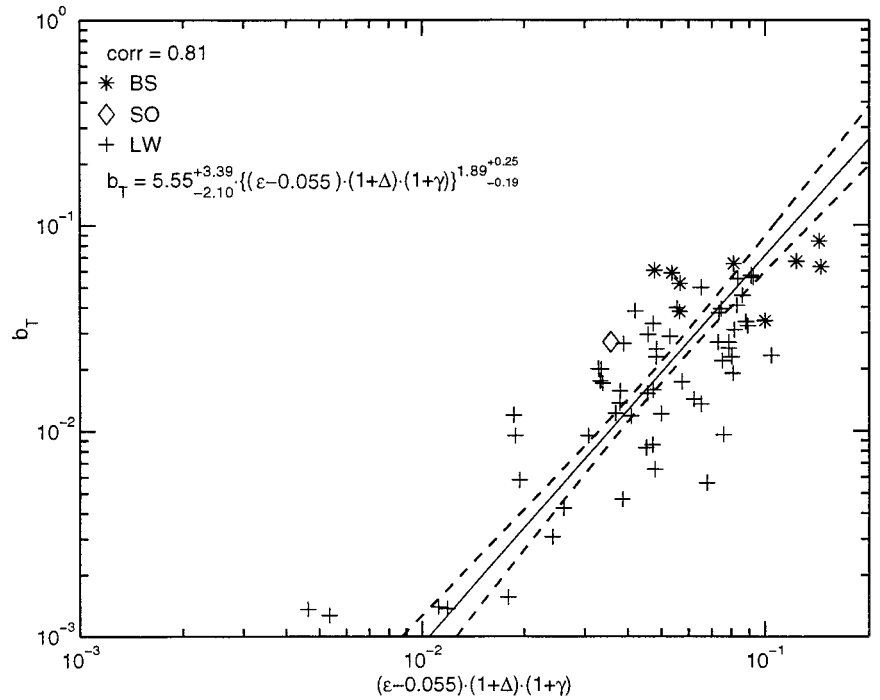

FIG. 7. As for Fig. 6 but plotted against the composite parameter $(\varepsilon - 0.055)(1 + \Delta)(1 + \gamma)$. The legend shows the correlation coefficient based on a linear best fit in the log–log domain, together with the coefficients at the ±90% confidence limits.

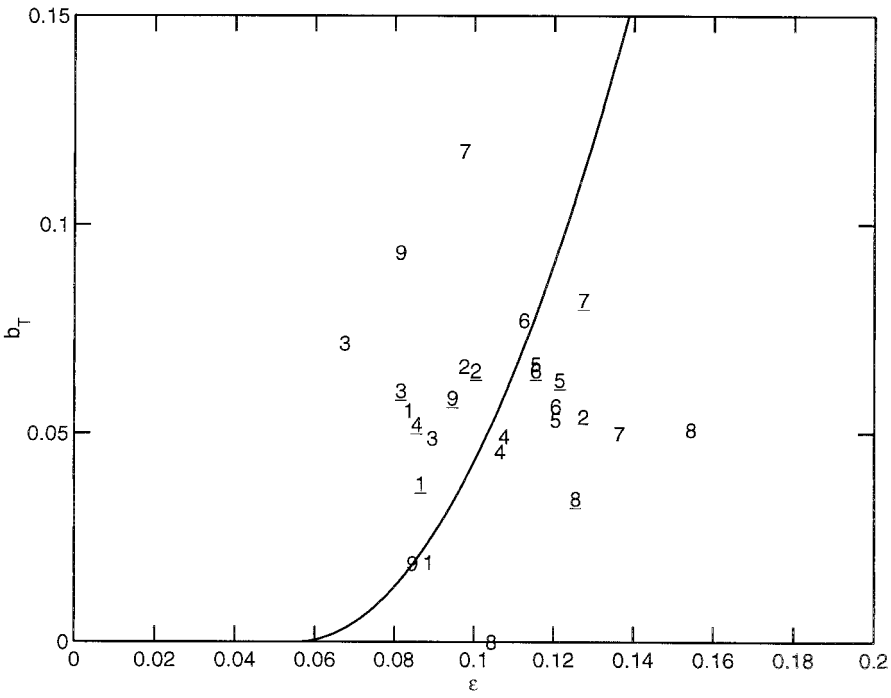

FIG. 8. The variability in a subset of the Black Sea data associated with record length. The nine experiments are listed in Table 1. For each experiment, there are three points shown; the underlined point is the 40-min average of the two nonunderlined 20-min average data points. The curve is the proposed correlation shown in the legend of Fig. 6.

parameters that vanishes when surface layer shear and wind input are absent. The correlation coefficient is marginally higher at 0.81, with a slightly reduced exponent and reduction of the overall error tolerance on the fitted parameters. This modest improvement is consistent with the notion of a secondary influence on breaking probability due to a superposed vertical shearing current and wind forcing in conjunction with the primary influence due to nonlinear intragroup modulation effects.

d. Note on long-term variability

An interesting result on the sensitivity of the correlation to the averaging time was found during our analysis of the Black Sea data. While 20-min records are usually regarded as sufficient for determining wave spectra, the number of wave groups required to provide stable breaking probabilities is found to be longer. The result of splitting several of the 40-min records into two 20-min records produced significantly more scatter in the dependence of b_T on ε. This scatter is shown in Fig. 8 for the nine cases identified in Table 1. Our limited duration data records and the relatively infrequent onset of dominant wave breaking did not allow us to further identify the source of this variability and future studies involving longer data records are clearly needed.

6. Frequency distributions of breaking events

A major motivation for studying breaking statistics is to refine the spectral dissipation source function for wind waves, as it is believed that most of the dissipation of wave energy takes place through wave breaking. This requires a reliable description of the probability of breaking events for different frequency or wavenumber bands in the wave spectrum and a quantification of the corresponding average amount of energy lost by the breakers in each spectral band.

Here, we present results of an initial study on the first of these issues, based on information gathered in the Black Sea dataset. We analyzed 2121 individual breakers in the 16 records listed in Table 1. The sampling frequency of 4 Hz allowed us to compile frequency distributions for the breakers as histograms over the range f_p to twice the peak frequency $2f_p$. Binning of breaking event probabilities was carried out for $\pm 15\%$ constant percentage wavenumber bands centered on k_p, $1.35k_p$, $1.83k_p$, $2.48k_p$, and $3.35k_p$, thereby covering the wavenumber range k_p to $4k_p$ or equivalently, the frequency range f_p to $2f_p$.

Figure 9 shows how the peak of the breaking probability distribution shifts from well above the spectral peak to close to the spectral peak as the dominant wave slope ε increases. This is consistent with the findings of Ding and Farmer (1994), who found from their rel-

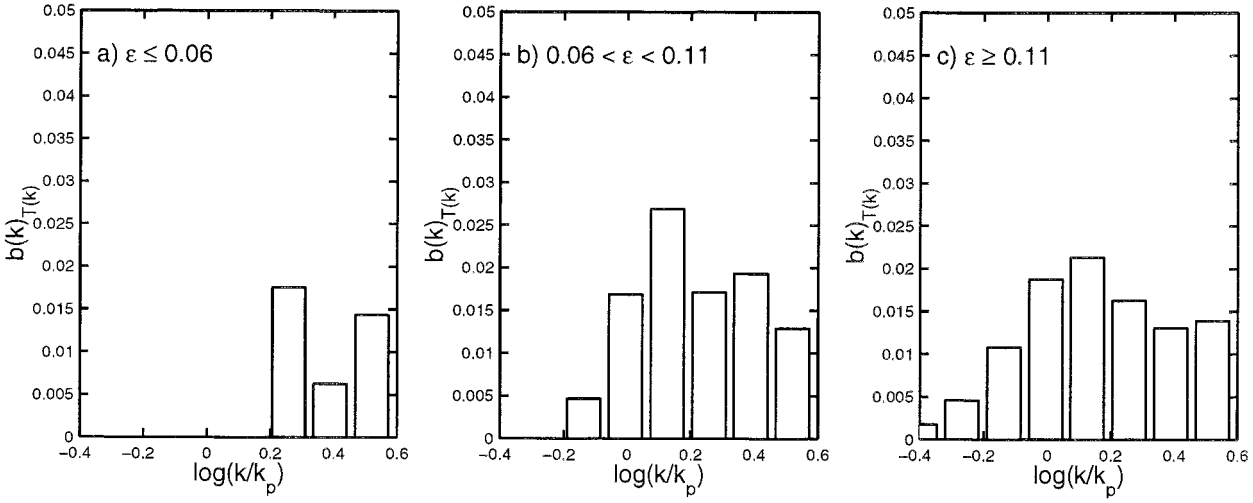

FIG. 9. The shift toward the spectral peak of the histogram of the breaking probability as a function of the mean steepness in each ±15% relative wavenumber bin (a) for $\varepsilon < 0.06$ (corresponding to well-developed seas); breaking occurs well above the spectral peak. For the steeper seas in (b) $0.06 < \varepsilon < 0.11$ and (c) $\varepsilon > 0.11$, the histogram peak moves toward the spectral peak.

atively old windsea conditions that the mean breaking event speed is considerably smaller than the phase speed of the dominant wind seas. It also follows the trend reported by Gemmrich and Farmer (1999), who observed that the peak of the normalised breaking frequency distribution was located well above the spectral peak frequency for typical mature windseas.

While negligible breaking is observed at the spectral peak for the wave fields with $\varepsilon < 0.06$, the wave breaking dissipation occurs at higher wavenumbers. This effect has been described as a wave age effect, but we point out that the breaking parameter ε is not unambiguously related to the wave age. Waves of the same nominal wave development stage U_{10}/c_p may have quite different values of ε due to a variety of mechanisms such as wave–swell and wave–current interactions. These could lead to different breaking probabilities at the spectral peak and different breaking frequency distributions for the same nominal wave age.

Plotting the same results in terms of the composite parameter $\varepsilon(1 + \Delta)(1 + \gamma)$ confirmed this behavior, showing an even stronger role of the spectral peak waves for high values of the composite parameter. These results are shown in Fig. 10.

Finally, we carried out an equivalent breaking probability dependence analysis to that made for the spectral peak region for a center frequency of $1.6 f_p$ (or $2.56 k_p$), using a ±30% relative frequency bandwidth. We noted

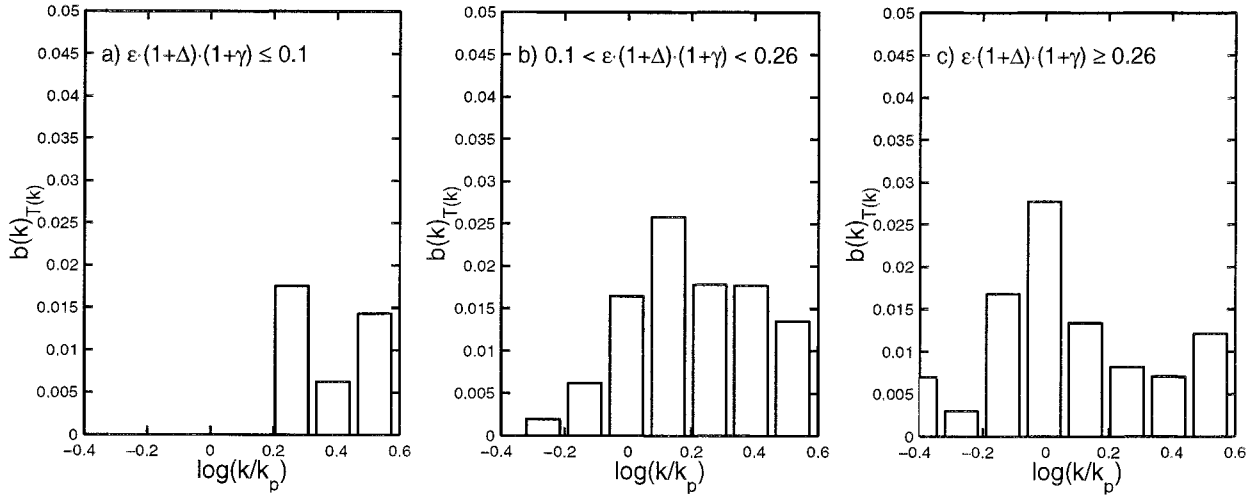

FIG. 10. As for Fig. 9 but in terms of the composite parameter $(\varepsilon - 0.055)(1 + \Delta)(1 + \gamma)$. These figures confirm the same shift seen in Fig. 9 toward the spectral peak of the histogram of the breaking probability as a function of the mean steepness in each ±15% relative wavenumber bin.

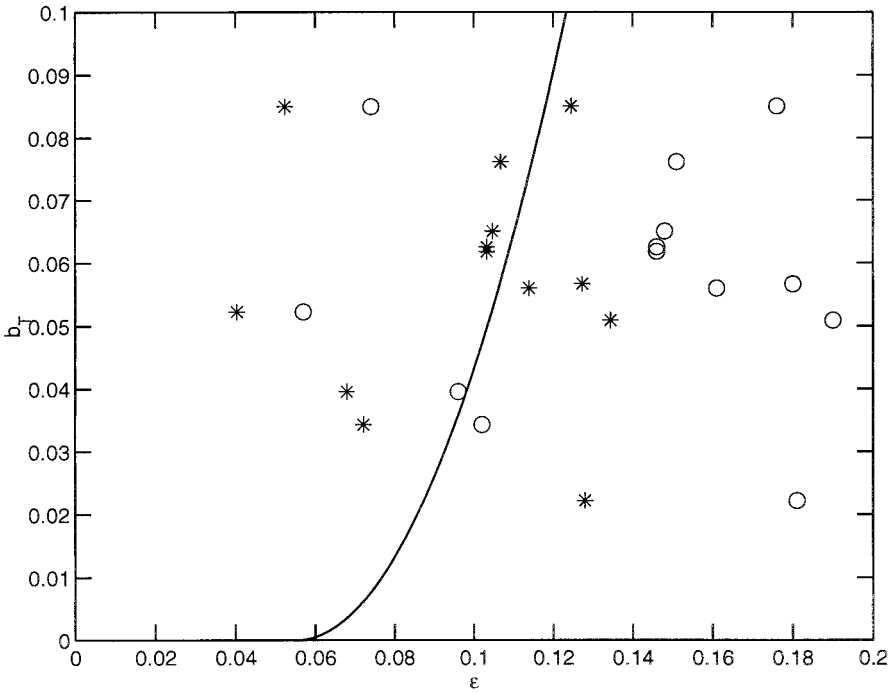

FIG. 11. Observed breaking probabilities in a (±30%) relative frequency band centered on $f_c = 1.6 f_p$ ($k_c/k_p = 2.56$) above the spectral peak. The breaking probabilities are referred to the center wave frequency in the band. The points shown (○) and (*) are respectively for a rectangular and triangular spectral window of width ±30% of f_c. The superimposed curve is the dependence of b_T on ε proposed for the dominant waves.

that because of the very different spectral shapes at the spectral peak (quasi-symmetrical) and above the spectral peak (rapidly decreasing with frequency), the use of (4.1) for higher wavenumber bands produced a mean slope measure with a significant bias. To reduce this bias, we investigated the use of the equivalent significant steepness

$$\varepsilon_s = 2\left[\int_{0.7f_c}^{1.3f_c} k^2 F(f)\, df\right]^{1/2}, \qquad (6.1)$$

where f_c is the center frequency of the band. While ε and ε_s agree within 10% for the spectral peak region, they can differ by more than 20% for higher wavenumber bands and (6.1) appears preferable for estimating the significant steepness for these bands. Based on this choice, our results for the band centered on $2.56k_p$ ($1.6f_p$) were calculated for a ±30% relative frequency bandwidth of $F(f)$, using a rectangular spectral window. These results for this higher wavenumber band are shown in Fig. 11. On the average, these results appear to lie to the right of our best-fit curve for the peak region. If we apply a spectral window with a triangular shape comparable with the spectral peak region (e.g., see Donelan et al. 1985, Fig. 11), this reduces the significant steepness estimates by a factor of $\sqrt{2}$. These results are also shown in Fig. 11 and appear to conform more closely to the breaking probability dependence on steepness found at the spectral peak. While this extension to higher wavenumber bands is speculative, we conclude that these data are not inconsistent with the dependence determined for the spectral peak region. There is clear evidence of a characteristic threshold behavior, and our data scatters about the superimposed breaking probability curve determined for the spectral peak. For this relatively limited dataset, the results from our initial analysis are encouraging and warrant further observational investigation. In this regard, we note that the issue of directional spreading will need to be addressed more closely in any future observational studies that extend to higher wavenumbers.

7. Conclusions

The traditional formulation of breaking probability of dominant ocean waves in terms of the wind speed shows very large scatter when applied to a broad range of wind wave conditions. The alternative breaking probability dependences proposed in this paper are based primarily on the spectral peak wave steepness. Minor refinement results from the inclusion of the influence of surface current shear and wind forcing strength, although wave breaking is less well correlated individually with these parameters. Our choice of spectral peak wave steepness as the primary independent variable was based directly on results of computations of evolution to breaking us-

ing a fully nonlinear free surface code by Dold and Peregrine (1986), Banner and Tian (1998), and from our more recent unpublished computations.

Using datasets from three sites that provided diverse wave scales, we determined a correlation for the breaking probability of the dominant waves in terms of the dominant wave steepness parameter ε. We found that the probability of breaking is zero, up to a threshold value of $\varepsilon = 0.055$ and then increases close to quadratically for $\varepsilon > 0.055$. The correlation coefficient for the wide range of wave scales investigated was 0.78. When the inferred secondary influences of vertical shear current and wind forcing were included in the parameterisation of spectral peak slope, the correlation improved marginally to 0.81. We note that our proposed dependence on mean ε is not a threshold criterion for breaking of individual waves, but represents an average wave field parameter for determining the mean fraction of breaking waves in the appropriate frequency band.

We also constructed frequency distributions of the breaking probabilities observed for wave frequencies above the spectral peak. These preliminary results indicate the following.

1) The peak of the breaking frequency distribution moves along the relative frequency f/f_p axis depending on the value of ε. For low values of ε, which often describe old seas, the peak in our data is located at approximately $1.6f_p$, while for higher values of ε, the peak shifts close to the spectral peak f_p. Thus for older wind seas, most breaking waves are shorter than the dominant waves, which may not break at all if their mean steepness stays below $\varepsilon = 0.055$. Since there are mechanisms operative (e.g., wave–current interactions) that can modify ε while the wave age remains constant, the proposed primary dependence of dominant wave breaking probability on hydrodynamic rather than aerodynamic variables is believed to be more fundamental.
2) Wave breaking probability data in a $\pm 30\%$ relative frequency spectral band centered at $1.6f_p$ are not inconsistent with the breaking probability threshold and quadratic dependence on spectral steepness found for the spectral peak waves. This provides encouraging initial support for extending the applicability of our view of dominant wave breaking to the breaking event distributions for higher frequency waves.

Overall, validation and refinement of this approach appears warranted. This requires further analysis of measurements of breaking probability using significantly longer observational records and consequently larger numbers of wave groups. This is left to future studies.

Acknowledgments. The authors gratefully acknowledge the financial support of the Australian Research Council and the U.S. Office of Naval Research. The authors also express their appreciation to A. I. Korovushkin, V. G. Proshchenko, Y. P. Soloviev, Y. N. Toloknov, and P. P. Verkeev for their assistance with the experiments in the Black Sea and are very grateful to Kristina Katsaros and Serhard Atakturk for providing access to the results of their breaking wave study on Lake Washington.

REFERENCES

Babanin, A. V., 1988: Connection of parameters of wind surface current with the wind in the North-West part of the Black Sea (in Russian, English abstract). *Morsk. Gidrofiz. Zh.,* **4,** 55–58.

——, 1995: Field and laboratory observations of wind wave breaking. *Second Int. Conf. on the Mediterranean Coastal Environment,* E. Ozhan, Ed., Autoritat Potuaria de Tarragona, Spain, **3,** 1919–1928.

——, and Y. P. Soloviev, 1998a: Field investigation of transformation of the wind wave frequency spectrum with fetch and the stage of development. *J. Phys. Oceanogr.,* **28,** 563–576.

——, and ——, 1998b: Variability of directional spectra of wind-generated waves, studied by means of wave staff arrays. *Mar. Freshwater Res.,* **49,** 89–101.

——, P. P. Verkeev, B. B. Krivinskii, and V. G. Proshchenko, 1993: Measurement of wind waves by means of a buoy accelerometer wave gauge. *Phys. Oceanogr.,* **4,** 387–393.

Banner, M. L., and D. H. Peregrine, 1993: Wave breaking in deep water. *Annu. Rev. Fluid Mech.,* **25,** 373–397.

——, and X. Tian, 1998: On the determination of the onset of wave breaking for modulating surface gravity water waves. *J. Fluid Mech.,* **367,** 107–137.

——, W. Chen, E. J. Walsh, J. Jensen, S. Lee, and C. B. Fandry, 1999: The Southern Ocean Waves Experiment. Part 1: Overview and mean results. *J. Phys. Oceanogr.,* **29,** 2130–2145.

Bass, S. J., and A. E. Hay, 1997: Ambient noise in the natural surf zone: Wave-breaking frequencies. *IEEE J. Ocean Eng.,* **22,** 411–424.

Craig, P. J., and M. L. Banner, 1994: Modeling wave-enhanced turbulence in the ocean surface layer. *J. Phys. Oceanogr.,* **24,** 2546–2559.

Ding, L., and D. M. Farmer, 1994: Observations of breaking surface wave statistics. *J. Phys. Oceanogr.,* **24,** 1368–1387.

Dold, J. W., and D. H. Peregrine, 1986: Water–wave modulations. *Proc. 20th Int. Conf. Coastal Eng.,* Taipei, Taiwan, ASCE, 163–175.

Donelan, M. A., M. S. Longuet-Higgins, and J. S. Turner, 1972: Whitecaps. *Nature,* **239,** 449–451.

——, J. Hamilton, and W. H. Hui, 1985: Directional spectra of wind-generated waves. *Philos. Trans. Roy. Soc. London,* **315A,** 509–562.

Gemmrich, J. R., and D. M. Farmer, 1999: Observations of the scale and occurrence of breaking surface waves. *J. Phys. Oceanogr.,* **29,** 2595–2606.

Hanson, J. L., and O. M. Phillips, 1999: Wind sea growth and dissipation in the open ocean. *J. Phys. Oceanogr.,* **29,** 1633–1648.

Hasselmann, K., and Coauthors, 1973: Measurements of wind-wave growth and swell decay during the Joint North Sea Wave Project (JONSWAP). *Dtsch. Hydrogr. Z.,* **A8** (Suppl.), No. 12, 95 pp.

Holthuijsen, L. H., and T. H. C. Herbers, 1986: Statistics of breaking waves observed as whitecaps in the open sea. *J. Phys. Oceanogr.,* **16,** 290–297.

Huang, N. E., 1986: An estimate of the influence of breaking waves on the dynamics of the upper ocean. *Wave Dynamics and Radio Probing of the Sea Surface,* O. M. Phillips and K. Hasselmann, Eds., Plenum, 295–313.

Jessup, A. T., C. J. Zappa, M. R. Loewen, and V. Hesany, 1997: Infrared remote sensing of breaking waves. *Nature,* **385,** 52–55.

Katsaros, K. B., and S. S. Atakturk, 1992: Dependence of wave-

breaking statistics on wind stress and wave development. *Breaking Waves*, M. L. Banner and R. H. J. Grimshaw, Eds., Springer, 119–132.

Kennedy, R. M., and R. L. Snyder, 1983: On the formation of whitecaps by a threshold mechanism. Part II: Monte Carlo Experiments. *J. Phys. Oceanogr.*, **13,** 1493–1504.

Kolaini, A. R., and M. P. Tulin, 1995: Laboratory measurements of breaking inception and post-breaking dynamics of steep short-crested waves. *Int. J. Offshore Polar Eng.*, **5,** 212–218.

Large, W. G., and S. Pond, 1981: Open ocean momentum flux measurements in moderate to strong winds. *J. Phys. Oceanogr.*, **11,** 324–336.

Longuet-Higgins, M. S., 1984: Statistical properties of wave groups in a random sea state. *Philos. Trans. Roy. Soc. London*, **312A,** 219–250.

——, 1986: Eulerian and Lagrangian aspects of surface waves. *J. Fluid Mech.*, **173,** 683.

——, and N. D. Smith, 1983: Measurement of breaking waves by a surface jump meter. *J. Geophys. Res.*, **14C,** 9823–9831.

Melville, W. K., M. R. Loewen, and E. Lamarre, 1992: Sound production and air entrainment by breaking waves: A review of recent laboratory experiments. *Breaking Waves*, M. L. Banner and R. H. J. Grimshaw, Eds., Springer, 139–146.

Millinazzo, F. A., and P. G. Saffman, 1990: Effect of surface shear stress layer on gravity and gravity–capillary waves of permanent form. *J. Fluid Mech.*, **216,** 93–101.

Nepf, H. M., C. H. Wu, and E. S. Chan, 1998: A comparison of two- and three-dimensional wave breaking. *J. Phys. Oceanogr.*, **28,** 1496–1510.

Papadimitrakis, Y. A., N. E. Huang, L. F. Bliven, and S. R. Long, 1988: An estimate of wave breaking probability for deep water waves. *Sea Surface Sound*, B. R. Kerman Ed., Kluwer, 71–83.

Pierson, W. J., and L. Moskowitz, 1964: A proposed spectral form for fully developed wind seas based on the similarity theory of S. A. Kitaigorodskii. *J. Geophys. Res.*, **69,** 5181–5190.

Rapp, R., and W. K. Melville, 1990: Laboratory measurements of deep water breaking waves. *Philos. Trans. Roy. Soc. London*, **331A,** 735–780.

She, K., C. A. Greated, and W. J. Easson, 1997: Experimental study of three-dimensional breaking kinematics. *Appl. Ocean Res.*, **19,** 329–343.

Snyder, R. L., and R. M. Kennedy, 1983: On the formation of whitecaps by a threshold mechanism. Part I: Basic formalism. *J. Phys. Oceanogr.*, **13,** 1482–1492.

——, L. Smith, and R. M. Kennedy, 1983: On the formation of whitecaps by a threshold mechanism. Part III: Field experiment and comparison with theory. *J. Phys. Oceanogr.*, **13,** 1505–1518.

Stokes, G. G., 1880: Considerations relative to the greatest height of oscillatory irrotational waves which can be propagated without change of form. *Math. Phys. Pap.*, **1,** 225–228.

Stolte, S., 1994: Short-wave measurements by a fixed tower-based and a drifting buoy system. *IEEE J. Oceanic Eng.*, **19,** 10–22.

Su, M. Y., A. W. Green, and J. Cartmill, 1996: Breaking wave statistics and near-surface microbubble density variations. *The Air–Sea Interface*, M. A. Donelan, W. H. Hui, and W. J. Plant, Eds., University of Miami Press, 303–308.

Teles Da Silva, A. F., and D. H. Peregrine, 1988: Steep, steady surface waves on water of finite depth with constant vorticity. *J. Fluid Mech.*, **195,** 281–302.

Terray, E. A., W. M. Drennan, and M. A. Donelan, 1999: The vertical structure of shear and dissipation in the ocean surface layer. *The Wind-Driven Air–Sea Interface*, M. L. Banner, Ed., The University of New South Wales, 239–245.

Thorpe, S. A., and P. N. Humphries, 1980: Bubbles and breaking waves. *Nature*, **283,** 463–465.

Toba, Y., and M. Chaen, 1973: Quantitative expression of the breaking of wind waves on the sea surface. *Rec. Oceanogr. Works Japan*, **12,** 1–11.

Weissman, M. A., S. S. Atakturk, and K. B. Katsaros, 1984: Detection of breaking events in a wind-generated wave field. *J. Phys. Oceanogr.*, **14,** 1608–1619.

Wu, J., 1979: Oceanic whitecaps and sea state. *J. Phys. Oceanogr.*, **9,** 1064–1068.

Xu, D., P. A. Hwang, and J. Wu, 1986: Breaking of wind-generated waves. *J. Phys. Oceanogr.*, **16,** 2172–2178.

Yuan, Y., C. C. Tung, and N. E. Huang, 1986: Statistical characteristics of breaking waves. *Wave Dynamics and Radio Probing of the Sea Surface*, O. M. Phillips and K. Hasselmann, Eds., Plenum, 262–272.